Super-high interlayer spacing of graphite oxide obtained by γ-ray irradiation in air

Hao Jin, Lei Chen, Kai Zheng, Zhiwei Xu, Jie Shi, Baoming Zhou, Mingjing Shan & Yinglin Li

Journal of Materials Science
Full Set - Includes `Journal of Materials Science Letters'

ISSN 0022-2461

J Mater Sci
DOI 10.1007/s10853-013-7766-y

Springer

J Mater Sci
DOI 10.1007/s10853-013-7766-y

Super-high interlayer spacing of graphite oxide obtained by γ-ray irradiation in air

Hao Jin · Lei Chen · Kai Zheng · Zhiwei Xu · Jie Shi · Baoming Zhou · Mingjing Shan · Yinglin Li

Received: 23 July 2013 / Accepted: 21 September 2013

Abstract We produced a type of graphite oxide with the interlayer spacing of 2.09 nm by treating conventional graphite oxide with γ-rays at an absorbed dose of 200 kGy in air. The expansion of interlayer distance should be attributed to the increased amounts of topological defects and then the improved steric hindrance between interlayers. Due to the decomposition of water molecules in graphite oxide by γ-rays, the reductive species were produced so that graphite oxide was partially reduced. It is also speculated to be the main mechanisms for alteration of oxygen groups. The change of carbon chain structures and oxygen groups were further supported by X-ray photoelectron spectroscopy, X-ray diffraction, and Fourier transform infrared spectroscopy. This simple and effective method of making graphite oxide with d-spacing of 2.09 nm by irradiating it in air is of interest not only for its easier intercalation and exfoliation than pristine one, but also for its potential to prepare graphene sheets with high percent of monolayers.

Introduction

Graphene, which has a single-atomic layered structure and unique mechanical [1], thermal [2], and electrical properties [3], is now enjoying significant attention for many technological applications. [4, 5] Recently, oxidation of natural graphite and subsequent chemical or thermal reduction of graphite oxide (GO) or graphene oxide [6–8] has been evaluated as one of the most efficient methods for low-cost and large-scale production of graphene. However, owing to the limited interlayer distance (with the biggest interlayer spacing of 0.95 nm in reported literatures) [9], it's hard to exfoliate GO exhaustively so that graphene sheets with high percent of monolayers cannot be produced successfully. Improving GO interlayer spacing has become an impressive subject we should pay close attentions to. Recently, many efforts have been committed to the intercalation of ions, molecules, and surfactants and the interlayer distance of GO was also proved to be increased [10–18]. Nevertheless, many substances are introduced into GO for the special applications such as catalysts, supercapacitor electrodes, and so on. In addition, this preparation process is not efficient enough for the large-scale production. Recent experiments have demonstrated that irradiation of carbon systems such as GO and graphene with energetic particles can be used to successfully modify their structures and performances [19–23]. γ-Ray irradiation, as a controllable method for modifying the physical and chemical properties of carbon systems, has attracted full attentions for their low-cost, large-scale, high-energy, and ultra-uniformity [24]. In our previous work, the interlayer spacing of multi-walled carbon nanotubes [25] and the performances of GO [26, 27] were manipulated by the γ-ray technique in small organic molecules. Herein, GO interlayer structures are proved to be changed by γ-irradiation in air. Furthermore, the alteration mechanisms were studied in detail.

H. Jin · L. Chen · Z. Xu (✉) · J. Shi · B. Zhou · M. Shan · Y. Li
Key Laboratory of Advanced Braided Composites, Ministry of Education, School of Textiles, Tianjin Polytechnic University, Tianjin 300160, People's Republic of China
e-mail: xuzhiwei@tjpu.edu.cn

K. Zheng
Zhangjiagang Entry-Exit Inspection & Quarantine Bureau, Zhangjiagang 215600, People's Republic of China

Published online: 01 October 2013

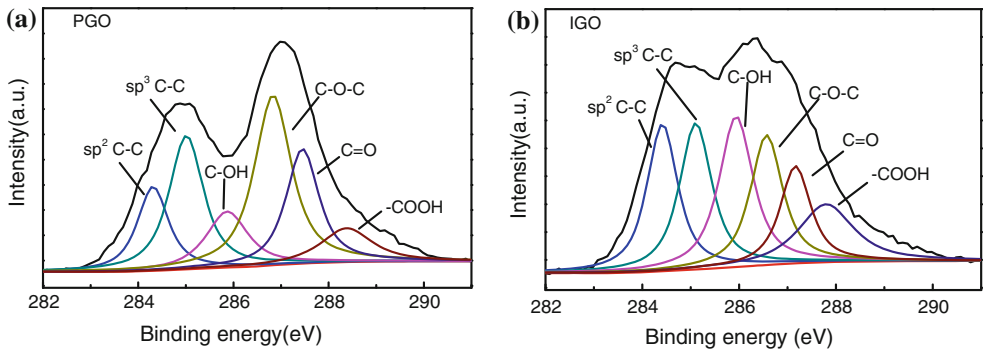

Fig. 1 C1s XPS spectra of **a** PGO and **b** IGO

Table 1 -Analysis of the deconvoluted C1s peaks from XPS and O/C of PGO and IGO

XPS C1s peaks	C1s fitting binding energy (eV; relative atomic percentage, %)						O/C
	C–C (sp^2)	C–C (sp^3)	C–OH	C–O–C	C=O	–COOH	
PGO	284.4 (14.33)	284.9 (15.59)	286.2 (10.96)	286.8 (31.41)	287.8 (19.65)	288.3 (8.05)	0.54
IGO	284.4 (19.39)	284.9 (20.20)	286.2 (20.73)	286.8 (16.89)	287.8 (12.76)	288.2 (10.03)	0.45

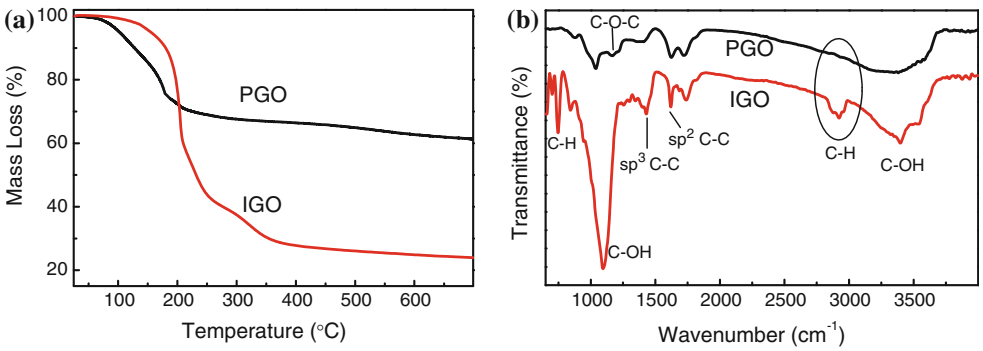

Fig. 2 **a** TG curves of PGO and IGO (in N_2) with a heating rate of 5 °C/min, and **b** FT-IR spectra of PGO and IGO

Experimental

The pristine GO (PGO) was prepared according to the method in [9]. The sample was exposed to ^{60}Co γ-ray source with an absorbed dose of 200 kGy in air at room temperature. The dose rate was 0.8 kGy/h. PGO and irradiated GO (IGO) were then characterized by X-ray diffraction (XRD, 1.54059 Å Cu Kα 1 as wavelength), X-ray photoelectron spectroscopy (XPS), Fourier transform infrared spectroscopy (FT-IR) spectra (Bruker VECTOR-22 IR spectrometer), and thermo gravimetric analyses (TGA). In addition, PGO and IGO were dispersed in deionized water under sonication for 2 h to get the nanosheets. The morphologies of them were analyzed by AFM (CSPM5500) and high resolution transmission electron microscope (HR-TEM, Tecnai G2 F20) observations. The UV–Vis absorption spectra of the dispersions were measured on a HITACHI UV-3310 spectrophotometer within the wavelength region 220–700 nm to evaluate the exfoliation of PGO and IGO in water.

Results and discussion

XPS was employed to determine the surface chemical composition of PGO and IGO. As shown in Fig. 1, curve fitting of PGO and IGO C1s spectra are performed using a Gaussian–Lorentzian peak shape and the results are recorded in Table 1. The C1 s of PGO and IGO both consist of six different chemically shifted components and can be deconvoluted into: sp^2 C–C, sp^3 C–C in aromatic rings (284.4 and 284.9 eV), C–OH (286.2 eV), C–O–C (286.8 eV), C=O (287.8 eV), and –COOH (288.3 eV). After γ-ray irradiation of GO, increased component for sp^2 C–C and sp^3 C–C can be observed. The ratio of O/C is also found to be decreased from 0.54 to 0.45 by irradiation (as

shown in Table 1). Both of these suggest partial decrease of the oxygen functional groups. To our knowledge, the high density of oxygen groups in PGO causes location of the water molecules between layers where they are attracted via hydrogen bonding [28]. According to the radiation chemistry of water [29], γ-ray irradiation can decomposed these water molecules to $^{\cdot}$OH and reductive (hydrogen radical and hydrated electron, $\dot{H}$ and e^{-}_{aq}) species, which can be used to create a medium for reducing PGO [30]. In addition, the increased C–OH and a decreased component for C–O–C can be obviously detected from Table 1. The C–O–C on the basal plane is unstable under the γ-rays. Bonding between ring-opening carbon-bear free radicals and $^{\cdot}$OH would make dramatic increase of C–OH. Moreover, these free radicals may bond with each other as well so that the amounts of sp^3 C–C are found to be increased obviously.

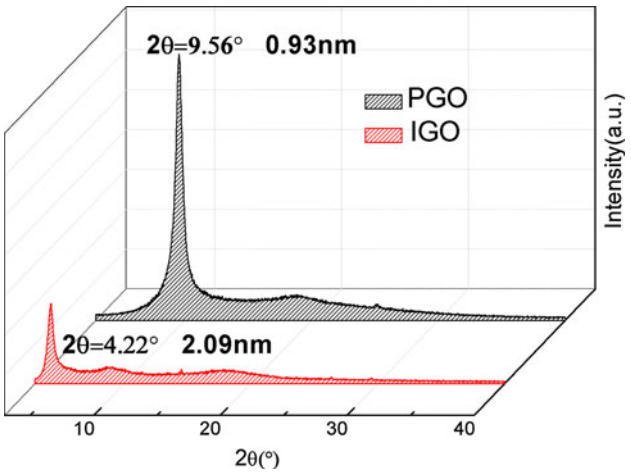

Fig. 3 Powder XRD patterns of PGO and IGO

TGA curves of PGO and IGO are shown in Fig. 2a. The weight of PGO starts to lose at around 90 °C, corresponding to the elimination of adsorbed water in PGO. After irradiation, the thermal stability of IGO below 180 °C is found to be obviously improved due to the fact that water molecules and thermally labile oxygen groups were prematurely decomposed by γ-rays in air. However, IGO has a bigger weight loss compared with that of PGO from 180 to 250 °C. This may be attributed to the fact that the amounts of –OH and –COOH are increased significantly in IGO, which would be decomposed below 250 °C so that more mass would be lost in IGO than PGO [31, 32]. FT-IR spectra of PGO (Fig. 2b) indicates the presence of sp^2 C–C at 1621 cm^{-1}, sp^3 C–C at 1433 cm^{-1}, C–O at 1218 cm^{-1}, and C–OH at 1060 and 3380 cm^{-1} [33]. After irradiation in air, the FT-IR spectrum of IGO exhibits characteristic vibration bands at 3000–2800 and 696 cm^{-1}, which is attributed to the stretching vibration of C–H, indicating the attachment of alkyl groups on the nanosheets by γ-ray irradiation. The characteristic peak at 1060 cm^{-1}, which is corresponded to alkoxy, is significantly increased by γ-rays. This should be caused by the bonding of carbon-bare free radicals with $\dot{H}$ or $^{\cdot}$OH. [30] In addition, the sp^3 C–C peaks become sharper, confirming the introduction of more topological defects in IGO.

The XRD patterns of PGO and IGO are shown in Fig. 3. The [001] peak of PGO shifts from 9.56° to 4.22° after γ-ray irradiation, which indicates the increase of PGO d-spacing from 0.93 to 2.09 nm. Probably, more topological defects that produced on IGO sheets (which were indicated by XPS and FT-IR results) and the increased steric hindrance in interlayers lead to the expansion [34, 35]. This significant increase in interlayer spacing makes IGO a promising candidate for the preparation of graphene sheets with high percent of monolayers due to the easier

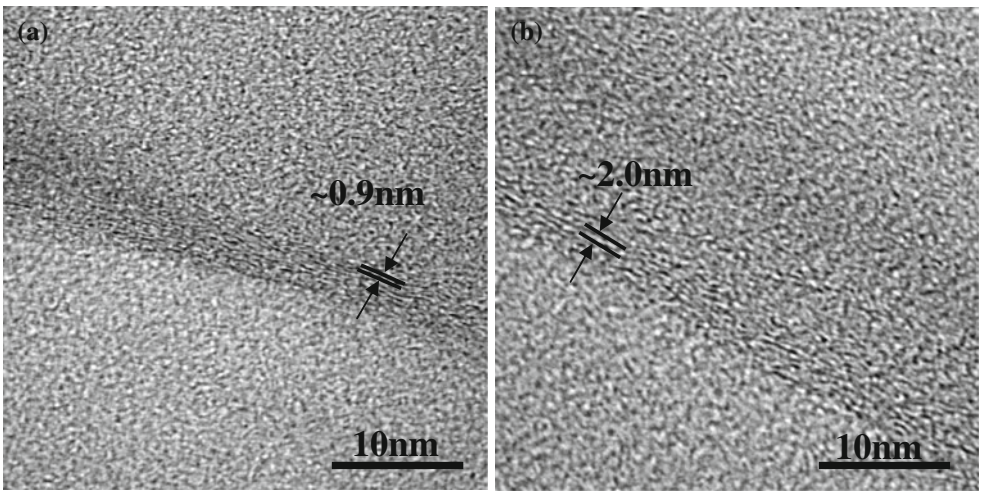

Fig. 4 HR-TEM images of **a** PGO and **b** IGO crinkles

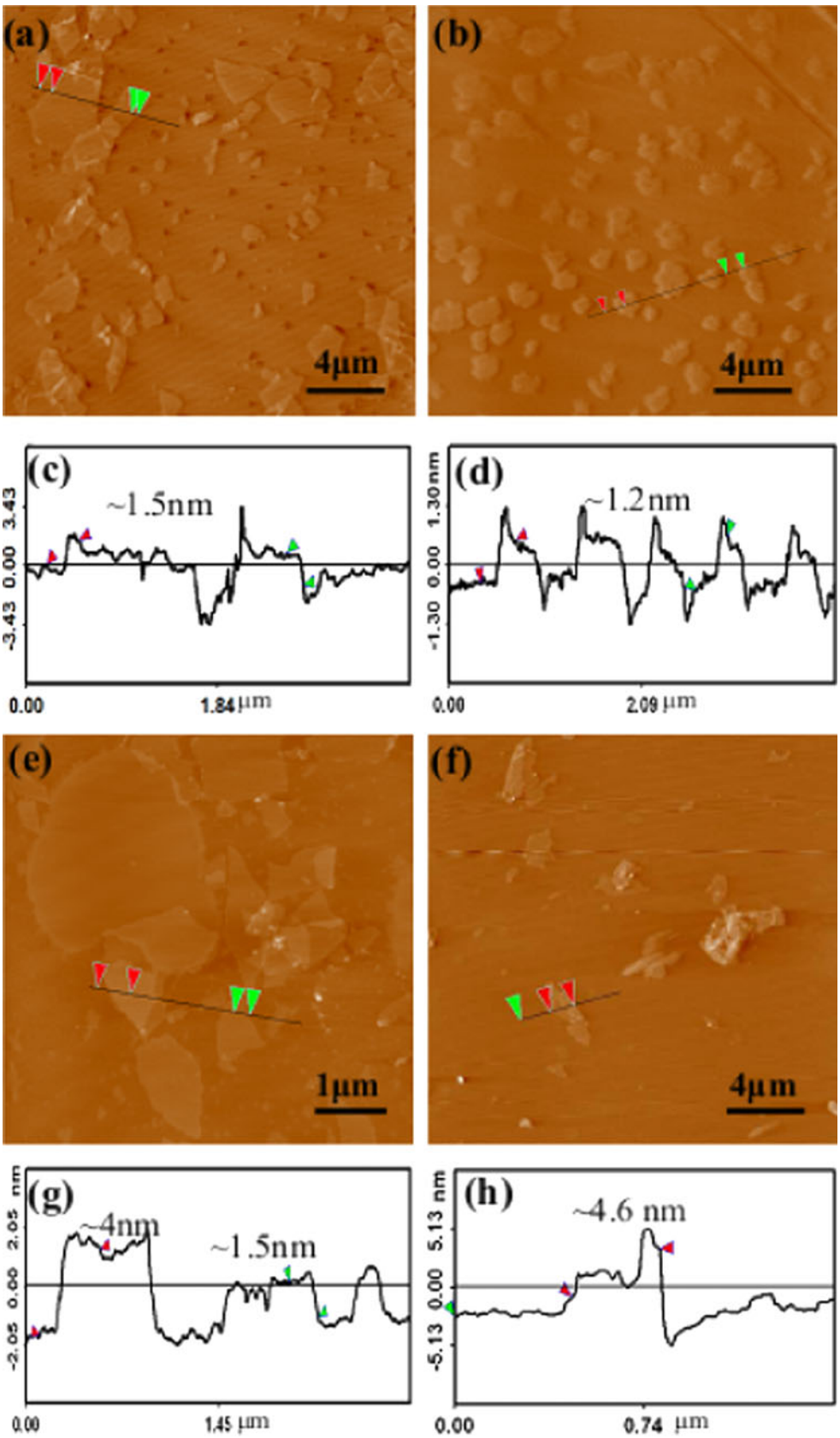

Fig. 5 Tapping mode of AFM topographic images of graphene nanosheets from sonicated **a** PGO and **b** IGO, and the cross-section of graphene nanosheets from **c** PGO and **d** IGO. To evaluate the thickness of the bi-layer sheets, **e**, **f** are the images for sonicated PGO and IGO, **g**, **h** are the corresponding heights

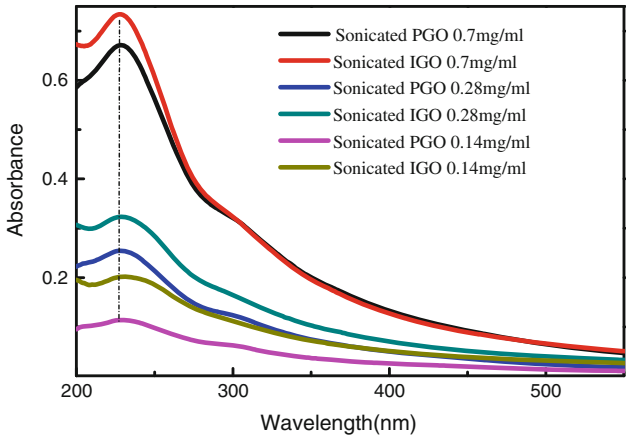

Fig. 6 UV–Vis spectra of PGO and IGO

exfoliation compared with that of PGO. The increase of d-spacing can also be observed by HR-TEM images of PGO and IGO. The crinkles of dissolved sheets were observed carefully to make sure this distance alteration. In Fig. 4, the interlayer distance of GO was found to be increased from ~0.9 to ~2.0 nm (see the insert), which was in good agreement with the speculation in XRD results. Moreover, the size of carbon domains was seemed to be different from each other, which should be attributed to the alteration of carbon chain structures and the increase of sp^3C–C.

AFM images of exfoliated PGO and IGO are presented in Fig. 5. The thickness of PGO single-layer sheet we prepared is 1.5 nm (Fig. 5a, c). Some graphene sheets are shown as multi-layers from Fig. 5a because of the overlapping or aggregation in sonicated PGO samples. However, after sonicating IGO, the monolayer percent is significantly increased and the nanosheets are found to be dispersed uniformly owing to the dramatic increase of d-spacing. Furthermore, it would be noteworthy that the height of the IGO sheets we obtain by γ-ray irradiation process is around 1.2 nm (Fig. 5b, d), thinner than monolayer PGO sheets. This could be a result of the dramatic decrease of epoxide groups on the basal PGO sheets [30]. To evaluate the exact d-spacing of PGO and IGO, the heights of the bi-layer PGO and IGO are also detected (Fig. 5e–h). In PGO, the thickness of bi-layer is about 4 nm, implying the d-spacing of 1 nm by deducting the thickness of two single-sheets. As well, the d-spacing of IGO can be calculated as 2.2 nm, which is in good agreement with the XRD results. It seems unbelievable that the thickness of the monolayer sheet is decreased while the interlayer distance of PGO is increased. We think that the whole amounts of oxygen groups are decreased, which bring about the decrease of monolayer thickness [9, 30]. Nevertheless, the interlayer distance of PGO is expanded due to the increase of topological defects and increased steric hindrance in interlayers [34, 35]. The actual mechanisms need to be further investigated in our later work.

In order to quantitatively assess the efficiency of improved d-spacing in exfoliating GO, UV–Vis spectroscopy is employed to detect the absorption of sonicated PGO and IGO solutions under the same concentrations. In Fig. 6, PGO and IGO both have a very similar λ_{max}, which is in the 227–231 nm range as previously reported for GO [36]. UV absorbance is solely due to the presence of dispersed nanomaterials, [37, 38] which means that a higher absorbance in UV–Vis spectra may be attributed to a better distribution of the materials under the same concentrations [38]. The absorbance of sonicated IGO is much higher than that of sonicated PGO in the same concentration, suggesting more extensive exfoliation of IGO than PGO due to the increased d-spacing by γ-ray irradiation.

Conclusions

The over onefold of increase in the PGO interlayer distance is achieved by irradiating GO with γ-rays in air. A significantly increased component for sp^3 C–C can be observed, which should be the main mechanisms for the increase of interlayer distance due to the increase of topological defects and then the enhanced steric hindrance between interlayers. The monolayer percent of the sonicated IGO is confirmed to be significantly increased from AFM due to the enlarged d-spacing. In addition, because of the extensive exfoliation of IGO, sonicated IGO sheets are dispersed more homogeneously than that of PGO, which is proved by UV–Vis spectra.

Acknowledgements The authors acknowledge the financial support from National Natural Science Foundation of China (11175130), Natural Science Foundation of Tianjin, China (10JCYBJC02300), and China Postdoctoral Science Foundation (2012M520578).

References

1. Lee C, Wei XD, Kysar JW, Hone J (2008) Science 321:385. doi:10.1126/science.1157996
2. Balandin AA, Ghosh S, Bao WZ et al (2008) Nano Lett 8:902. doi:10.1021/nl0731872
3. Novoselov KS, Morozov SV, Mohinddin TMG et al (2007) Phys Status Solidi B 244:4106. doi:10.1002/pssb.200776208
4. de Guzman RC, Yang J, Ming-Cheng M, Salley SO, Ng KYS (2013) J Mater Sci 48:4823. doi:10.1007/s10853-012-7094-7
5. Han Y, Wu Y, Shen M, Huang X, Zhu J, Zhang X (2013) J Mater Sci 48:4214. doi:10.1007/s10853-013-7234-8
6. Rourke JP, Pandey PA, Moore JJ et al (2011) Angew Chem Int Ed 50:3173. doi:10.1002/anie.201007520
7. Wilson NR, Pandey PA, Beanland R et al (2009) ACS Nano 3:2547. doi:10.1021/nn900694t

8. Thomas HR, Valles C, Young RJ, Kinloch IA, Wilson NR, Rourke JP (2013) J Mater Chem C 1:338. doi:10.1039/c2tc00234e
9. Marcano DC, Kosynkin DV, Berlin JM et al (2010) ACS Nano 4:4806. doi:10.1021/Nn1006368
10. Hu ZL, Aizawa M, Wang ZM, Hatori H (2009) Carbon 47:3377. doi:10.1016/j.carbon.2009.08.008
11. Wang R, Sun J, Gao L, Xu C, Zhang J (2011) Chem Commun 47:8650. doi:10.1039/c1cc11488c
12. Mastalir A, Kiraly Z, Patzko A, Dekany I, L'Argentiere P (2008) Carbon 46:1631. doi:10.1016/j.carbon.2008.06.054
13. Gotoh K, Kinumoto T, Fujii E et al (2011) Carbon 49:1118. doi:10.1016/j.carbon.2010.11.017
14. Matsuo Y, Nishino Y, Fukutsuka T, Sugie Y (2007) Carbon 45:1384. doi:10.1016/j.carbon.2007.03.037
15. Zhang K, Mao L, Zhang LL, Chan HSO, Zhao XS, Wu J (2011) J Mater Chem 21:7302. doi:10.1039/c1jm00007a
16. Matsuo Y, Hatase K, Sugie Y (1998) Chem Mater 10:2266. doi:10.1021/cm980203a
17. Matsuo Y, Niwa T, Sugie Y (1999) Carbon 37:897. doi:10.1016/s0008-6223(98)00226-7
18. Liu ZH, Wang ZM, Yang XJ, Ooi KT (2002) Langmuir 18:4926. doi:10.1021/la011677i
19. Baraket M, Walton SG, Wei Z, Lock EH, Robinson JT, Sheehan P (2010) Carbon 48:3382. doi:10.1016/j.carbon.2010.05.031
20. Zhang Y, Ma H-L, Zhang Q et al (2012) J Mater Chem 22:13064. doi:10.1039/c2jm32231e
21. Chen WF, Zhu ZY, Li SR, Chen CH, Yan LF (2012) Nanoscale 4:2124. doi:10.1039/c2nr00034b
22. Kai S, Xiaoying Z, Yueming X, Hewen L (2013) J Mater Sci 48:5750. doi:10.1007/s10853-013-7367-9
23. Min Y, He G, Xu Q, Chen Y (2013) Dalton Trans 42:12284. doi:10.1039/c3dt51498f
24. Xu ZW, Chen L, Zhou BM et al (2013) RSC Adv 3:10579. doi:10.1039/c3ra00154g
25. Xu ZW, Chen L, Liu LS, Wu XQ (2011) Carbon 49:350. doi:10.1016/j.carbon.2010.09.023
26. Chen L, Xu Z, Li J et al (2012) J Mater Chem 22:13460. doi:10.1039/C2JM31208E
27. Zhang Y, Chen L, Xu Z et al (2012) Mater Lett 89:226. doi:10.1016/j.matlet.2012.08.113
28. Stankovich S, Dikin DA, Piner RD et al (2007) Carbon 45:1558. doi:10.1016/j.carbon.2007.02.034
29. Anderson AR, Hart EJ (1962) J Phys Chem 66:70. doi:10.1021/j100807a014
30. Zhang BW, Li LF, Wang ZQ et al (2012) J Mater Chem 22:7775. doi:10.1039/c2jm16722k
31. Bagri A, Mattevi C, Acik M, Chabal YJ, Chhowalla M, Shenoy VB (2010) Nat Chem 2:581. doi:10.1038/nchem.686
32. Wang GC, Yang ZY, Li XW, Li CZ (2005) Carbon 43:2564. doi:10.1016/j.carbon.2005.05.008
33. Zhou XJ, Zhang JL, Wu HX, Yang HJ, Zhang JY, Guo SW (2011) J Phys Chem C 115:11957. doi:10.1021/jp202575j
34. Hummer WS, Offeman R (1958) J Am Chem Soc 80:1339. doi:10.1021/ja01539a017
35. Compton OC, Nguyen ST (2010) Small 6:711. doi:10.1002/smll.200901934
36. Li D, Muller MB, Gilje S, Kaner RB, Wallace GG (2008) Nat Nanotechnol 3:101. doi:10.1038/nnano.2007.451
37. Pan YZ, Bao HQ, Li L (2011) ACS Appl Mater Interfaces 3:4819. doi:10.1021/am2013135
38. Shim SH, Kim KT, Lee JU, Jo WH (2012) ACS Appl Mater Interfaces 4:4184. doi:10.1021/am300906z